

Multi-objective Topology Optimization Design for a Certain Launcher Bracket

Yue Ma¹, Qilin Shu¹*, Longjun Tan¹, Yuekang Yue², Chen Tian³

¹Shenyang Ligong University, School of Mechanical Engineering, Shenyang 110159, China

²Shanghai Donghu Machinery Factory, Shanghai 201900, China

³Beijing Zhongke Aerospace Talent Service Co., LTD. Jiangsu branch, Nanjing 210000, China

*Correspondence: shuqilin@sylu.edu.cn

Abstract: To achieve weight reduction and enhance the firing accuracy of a specific type of launch device, the bracket was selected as the optimization subject for multi-objective topology optimization. Single-objective optimization often overlooks other influencing factors. To address the limitations of single-objective optimization, this study adopts the variable density method from the SIMP approach and proposes a multi-objective topology optimization based on compromise programming. This study, through multi-objective topology optimization of the bracket, obtained an optimized topology structure that maximizes static stiffness and the dynamic low-order natural frequencies of the launch device bracket at launch angles of 0°, 53°, and 85°, with an azimuth angle of 0°. Finally, the obtained topology structure was validated using finite element software. The design method presented in this paper not only enhanced the stiffness of the bracket structure for such launch devices and increased the first two natural frequencies of the bracket but also achieved weight reduction. The optimization design process also provides a reference for other mechanical structures.

Keywords: Bracket; Topology optimization; Multi-objective; Compromise Programming method.

How to cite this paper:

Ma, Y., Shu, Q., Tan, L., et al. Multi-objective Topology Optimization Design for a Certain Launcher Bracket. *Innovation & Technology Advances*, 2024, 2(2), 46–58. <https://doi.org/10.61187/ita.v2i2.118>

1. Introduction

The bracket is the main support structure of the launcher, bearing the recoil generated during the launch process, and serving as the foundation for the installation of other structural components and equipment of the launcher. The bracket, situated between the launch box and the gear seat ring, serves as the primary rotor of the launcher. Various electrical drive components, such as the height adjuster and the launch box, are mounted on the bracket and rotate with it, facilitating the launching process. To ensure the accuracy of the launcher, the rigidity and natural frequency of the bracket must be carefully considered.

Topology optimization is the analysis of finite element models with established loads and boundary conditions, aiming to achieve optimal material distribution through specified constraints and objective functions, thereby obtaining optimized design solutions. Single-objective optimization remains the mainstream approach in topology optimization currently. With the further improvement of modern engineering's requirements for mechanical quality, optimization is no longer just about a single objective, and the demand for multi-objective optimization design is increasing. Under static conditions, the inherent frequencies under multiple operating conditions are important parameters of stiffness and dynamic conditions, and their multi-objective topology optimization is a common challenge in the engineering field.

Su Changqing et al. employed the compromise programming method to maximize dynamic vibration frequencies and static stiffness under multiple loading conditions, when conducting topology optimization of aircraft engine mounts [1]. Pan Xixi et al.



Copyright: © 2024 by the authors. Submitted for possible open access publication under the terms and conditions of the Creative Commons Attribution (CC BY) license (<http://creativecommons.org/licenses/by/4.0/>).

adopted a weighted compromise programming method to propose a comprehensive objective function that includes natural frequency and compliance. This approach achieved an optimal balance of dynamic natural frequencies and static stiffness for the common base of a certain type of marine diesel-electric element, addressing the issue of natural frequencies being close to the excitation frequencies of the diesel engine [2]. Sun Xiaohui et al. weighting method and compromise programming method, to establish five distinct objective functions. The results demonstrated that all five methods could address multi-objective topology optimization problems. Among them, the linear weighting method contributed significantly to improving structural stiffness, while the compromise programming method was more effective in enhancing the natural frequencies of the structure [3]. Li Wenhua et al. proposed a local convergence indicator (ILC) and designed an environmental selection strategy based on this indicator and improved population crowding. Based on this, they introduced a multi-modal multi-objective optimization algorithm for obtaining global and local optimal solution sets [4]. Cui Yupeng et al. proposed a method based on compromise programming and an improved game theory quadruple combination weighting method. Utilizing the IFCWGT strategy, which integrates the game theory idea of non-preferential coupled analytic hierarchy process, entropy weighting method, inter-layer correlation method, and coefficient of variation method, they enhanced the topology performance and layout of open decks [5]. Lan Fengchong et al. used compromise programming to define a comprehensive objective function for maximizing static stiffness and the first-order modal frequency of a steering knuckle under multiple loading conditions. This approach significantly improved the stiffness and first-order modal frequency of the steering knuckle while reducing its weight [6]. Ge Shicheng applied the compromise programming method to define a multi-objective topology optimization function for static stiffness and dynamic vibration frequency, resulting in a topology structure that simultaneously meets the requirements for no-load stiffness, load compliance, and low-order vibration frequencies of flexible mechanisms [7]. Fan Wenjie et al. employed the compromise programming method for multi-objective topology optimization of a vehicle frame structure, effectively enhancing the stiffness and natural frequencies of the frame and improving its overall performance [8]. Xiang Weicheng et al., in order to obtain a naval gun bracket with maximum stiffness and dynamic frequency under multiple firing angles, used the compromise method to normalize and dimensionless multiple objectives, resulting in a validated bracket optimization model [9]. Zhou Yu, et al. utilized a normalized decision-making algorithm to obtain the optimal compromise solution from the Pareto set of multiple objectives [10]. Zaifang Zhang, et al. obtained the optimal hydraulic loading structure of tank bottom by using multi-objective particle swarm optimization algorithm [11]. Haris Moazam Sheikh et al. proposed the MixMOBO method, which can identify multiple effective Pareto solutions, addressing the issue that traditional Bayesian methods cannot handle multi-objective variables [12]. Junyuan Zhang, et al. proposed a topology optimization method for castings, establishing constraint equations for casting formation based on the vector method. The component baseline is proposed to realize automatic filtering. This method optimizes the structure without cavities, enhancing its manufacturability [13].

2. Simp Method

Structural topology optimization can be regarded as determining the necessity of the presence of a material in a certain element within the unfrozen region, where the material's elastic modulus function varies with the relative density of the elements in the density-based method. It aims to determine the sensitivity of the structural stiffness to the relative density of each element, retaining sensitive elements while removing insensitive ones. However, solving discrete problems computationally is not convenient. Therefore, they are usually transformed into continuous problems for research. The density-based method is based on this research idea, and after verification of its feasibility, it has been

widely applied in practice. The density-based method utilizes a continuously varying density function as the independent variable, and employs a given mapping function to derive the relationship between the macroscopic elastic modulus of the material and the relative density of the element. It assumes isotropic material properties and does not involve microstructural or additional homogenization processes. Utilizing the computational power of computers enables the optimization process to be both scientific and efficient [14-16].

The SIMP method is an extension of the aforementioned density-based method. Based on the aforementioned, the SIMP method accelerates the convergence of material elements towards either "existence" or "non-existence" by introducing a penalty factor during optimization iterations [17]. Assuming that the relative density of the element after iteration and the elastic modulus of the material remain isotropic, while the value of Poisson's ratio remains unchanged, the mathematical equation for constructing the material interpolation model using the SIMP method defines as:

$$\begin{cases} E_i(x)/E^0 = x_i^p \\ 0 \leq x \leq 1 \end{cases} \quad (1)$$

In formula 1: $E_i(x)$ is the relative elastic modulus in the iterative process, i is the optimized element number, E^0 is the true elastic modulus of the material, and $E_i(x)$ has a value between 0 and E^0 : when $E_i(0)=0$, $E_i(1)=E^0$. x is the relative density of the element, and p is the introduced penalty factor. The value rule of the penalty factor p of the entity element is as:

$$p \geq \max \left\{ 15 \frac{1-\nu_0^2}{7-5\nu_0^2}, 1.5 \frac{1-\nu_0^2}{1-2\nu_0^2} \right\} \quad (2)$$

In formula 2: ν_0 is the Poisson ratio of the material.

The optimization model constructed by SIMP method is written as:

$$\begin{cases} \text{find } x = (x_1, x_2, \dots, x_n)^T \\ \min C(x) = F^T U = U^T K U \\ \text{s.t. } V(x) = \sum_{i=1}^n x_i v_i \leq a \Omega \end{cases} \quad (3)$$

In formula 3: x is the design variable, n is the number of design variables, $C(x)$ is the target to be optimized, F is the load vector on the node, U is the displacement vector of each node, and K is the stiffness matrix of the structure. Ω is the non-frozen area, a is the percentage of the optimized structure volume V in the non-frozen area Ω in the original bracket volume, v_i is the volume of the element.

The deficiencies of the SIMP method are as follows: although utilizing penalization factors effectively drives the relative density of the elements towards 0 or 1, thereby reducing the number of elements with intermediate densities, the optimized checkerboard phenomenon and the instability of pseudo-density values still persist. Moreover, the outcomes of topology optimization based on the iterative structure topology of the SIMP method are not solely dependent on the penalization factor (p), but also on the mesh division of the finite element model. This limitation can be mitigated by integrating optimization constraints such as minimum (maximum) member size constraints, independent point density interpolation methods, density slope methods, and perimeter constraints with the SIMP method.

3. Multi-Objective Function for Topology Optimization of Bracket Structure

3.1. Objective Function of Static multi-condition Stiffness Topology Optimization

The multi-stiffness topology optimization refers to the optimization scenario where stiffness is the optimization objective under multiple loading conditions, which is a type of multi-objective topology optimization problem. Methods such as linear weighting, square weighting, normative objective, shortest distance, and compromise programming can all be employed to solve multi-objective problems. Under different operating conditions, the stiffness of the bracket structure is linearly weighted since it represents the same characteristic. Therefore, normalization is unnecessary, allowing the resolution of multi-load cases to be transformed into solving single-load case problems directly. In the past, the linear weighting method was commonly employed to solve multi-stiffness optimization problems. In improving the comprehensive stiffness under multiple operating conditions, the impact is significant. However, if the linear weighting method is simply employed, for non-convex optimization problems, where there are multiple objectives with different elements or there exists a coupled relationship with negative correlation between multiple objectives, the optimal solution for multiple objectives cannot be simultaneously achieved. Due to the difference in dimensionalities and magnitudes between the inherent frequency and structural stiffness, a generalized approach similar to normalization is considered for their joint solution. According to the requirements stated above, compromise programming applies normalization to the scale of the optimization objectives and demonstrates a favorable effect on improving the inherent frequencies of structures. Therefore, this paper addresses the comprehensive optimization problem of multi-stiffness trusses and dynamic frequencies using the method of compromise programming.

In the process of structural optimization, when addressing the problem of achieving maximum stiffness in structures under multiple loading conditions, the common objective is to attain the minimum compliance of the structure under these conditions. According to the principle of minimum potential energy, the maximum stiffness of the structure can be obtained by solving for the minimum strain energy. Therefore, the topology optimization of structures under multiple loading conditions, with the objective function being the minimum strain energy, is expressed using the compromise programming method as:

$$\min C(x) = \left\{ \sum_{k=1}^m w_k^q \left[\frac{C_k(x) - C_k^{\min}}{C_k^{\max} - C_k^{\min}} \right]^q \right\}^{\frac{1}{q}} \tag{4}$$

In formula 4: m represents the total number of load conditions; w_k represents the weight of the k -th sub-loading condition; q represents the penalty factor, $q \geq 2$; $C_k(x)$ represents the expression of the objective function of strain energy under the k -th sub-loading condition. C_k^{\max} and C_k^{\min} respectively represent the maximum and minimum values of the strain energy objective function under the k -th sub-loading condition.

3.2. Objective Function of Dynamic Natural Frequency Topology Optimization

In conventional modal frequency topology optimization methods, the volume fraction or mass fraction of the structure is typically constrained within a certain range, and the natural frequencies close to the working frequency of the structure are optimized to move them further apart. However, when using this method to increase the natural frequencies of certain orders, the modes of non-optimized orders may decrease due to changes in the structure, leading to the phenomenon of mode swapping among natural frequencies. To prevent this situation, this paper represents the optimization objective function by using the weighted average frequency of the natural frequencies of the orders to be optimized:

$$\max_{x=\{x_1, x_2, \dots, x_n\}} \Lambda(x) = \lambda_0 + s \left(\sum_{i=1}^f \frac{w_i}{\lambda_i - \lambda_0} \right)^{-1} \tag{5}$$

Specifically, the symbol $\Lambda(x)$ in the formula is the average frequency, λ_i represents the characteristic frequency of order i , λ_0 and s are known or given parameters, w_i is the weight coefficient of the frequency of order i , and f represents the order of the natural frequency to be optimized.

The advantage of defining the average frequency is that it takes into account the natural frequencies to be optimized within the formula. Even if the natural frequencies of the structure swap, the continuity of the average frequency formula remains relatively smooth due to the lack of abrupt changes in the structure during the optimization process.

3.3. Determination of Weights for Sub-objectives

The concept of satisfaction is introduced within the context of optimization problems to evaluate the degree of satisfaction with the optimization results throughout the iterative process. Satisfaction is denoted by the symbol q . When the optimization results are fully satisfactory, q is assigned a value of 1. Conversely, when the optimization results are completely unsatisfactory, q is assigned a value of 0. For levels of satisfaction that fall between fully satisfactory and completely unsatisfactory, q takes on values within the range of 0 to 1. **Figure 1** illustrates the satisfaction curve for the k -th sub-loading condition.

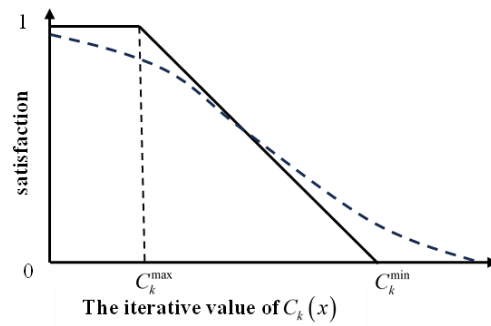


Figure 1. Three-Bend Satisfaction Curve and S-Shaped Satisfaction Curve

In the figure: the horizontal axis represents the iterative optimization results of the objective, and the vertical axis represents the satisfaction with the optimization results of the objective. C_k^{\min} represents the best optimization result for the k -th sub-loading condition. C_k^{\max} represents the worst optimization result for the k -th sub-loading condition.

The expression for the S-Shaped satisfaction curve is:

$$q_k = \frac{1}{1 + \exp\left(2 - 4 \frac{C_k(x) - C_k^{\min}}{C_k^{\max} - C_k^{\min}}\right)} \tag{6}$$

In formula 6: as $C_k(x)$ approaches C_k^{\min} , q_k approaches 1; as $C_k(x)$ approaches C_k^{\max} , q_k approaches 0.

The introduction of the satisfaction function avoids the need for manually selecting the weights for each sub-loading condition, allowing for dynamic iteration of the weights assigned to the objectives of each sub-loading condition. The expression for the weight coefficient of the k -th sub-loading condition is:

$$w_k = \frac{1 - q_k}{\sum_{k=1}^m (1 - q_k)} \tag{7}$$

In formula 7: q_k represents the satisfaction with the objective value $C_k(x)$ of the k -th sub-loading condition, while $1 - q_k$ represents the dissatisfaction with the objective

value $C_k(x)$ of the k -th sub-loading condition. The lower the satisfaction with $C_k(x)$, i.e., the greater the dissatisfaction with $C_k(x)$, the larger the value of w_k becomes, thereby increasing its influence on the overall objective and accelerating the achievement of a satisfactory value for $C_k(x)$. By dynamically adjusting w_k , each sub-objective is regulated to yield a satisfactory result.

3.4. Implementation of Compromise Optimization for Bracket Structures Based on Multi-Objective Optimization

The above sections have separately considered the multi-stiffness and low-order natural frequencies of the structure. Now, by integrating the compromise programming of the average natural frequency and multi-stiffness into a single formula and performing a weighted summation of these two different categories of objectives, we derive a comprehensive expression for the objective function that simultaneously optimizes both the multi-stiffness and the frequencies.

$$\min F(x) = \left\{ w^2 \left[\sum_{k=1}^m w_k \frac{C_k(x) - C_k^{\min}}{C_k^{\max} - C_k^{\min}} \right]^2 + (1-w)^2 \left(\frac{\Lambda_{\max} - \Lambda(x)}{\Lambda_{\max} - \Lambda_{\min}} \right)^2 \right\}^{\frac{1}{2}} \quad (8)$$

Where, $F(x)$ represents the comprehensive objective function expression; w represents the weight of the weighted strain energy objective function under multiple loading conditions. w_k represents the weight of the k -th sub-loading condition; $C_k(x)$ represents the flexibility of the k -th sub-loading condition; C_k^{\max} and C_k^{\min} represent the maximum strain energy and minimum strain energy of the structure under the k -th sub-loading condition respectively. Λ_{\max} and Λ_{\min} are the maximum and minimum values of the frequency objective function respectively. $\Lambda(x)$ is the average frequency.

In this paper, the proposed compromise programming formula and the integrated formula of average frequency are defined within the custom functions provided by finite element software. These are set as function responses, with the volume response given as a constraint condition. Finally, the custom function response is used as the objective for topology optimization.

4. Establishment of Multi-Objective Structure Optimization Model of Bracket

4.1. Simulation Conditions

To reduce the difficulty of mesh generation in the preprocessing stage, features that have a minimal impact on the analysis, such as chamfers and round holes, were removed while retaining essential structural features. The simulation conditions defined in this paper are shown in **Table 1**. Two extreme launch angles and one common launch angle were selected for analysis, with other launch angles temporarily disregarded.

Table 1. Simulation conditions

load cases	specification
CASE1	The emission Angle is 0° and the directional emission Angle is 0°
CASE2	The emission Angle is 53° and the directional emission Angle is 0°
CASE3	The emission Angle is 85° and the directional emission Angle is 0°

4.2. Dynamic Simulation

Using Adams software, dynamic modeling simulations of the launching device under three conditions were conducted, yielding the maximum instantaneous recoil force

between the launch box and the bracket trunnion for each condition. The maximum instantaneous recoil force of 200 KN obtained from the analysis is used as the load that the optimized bracket structure must withstand. The specific models are shown in **Figure 2**.

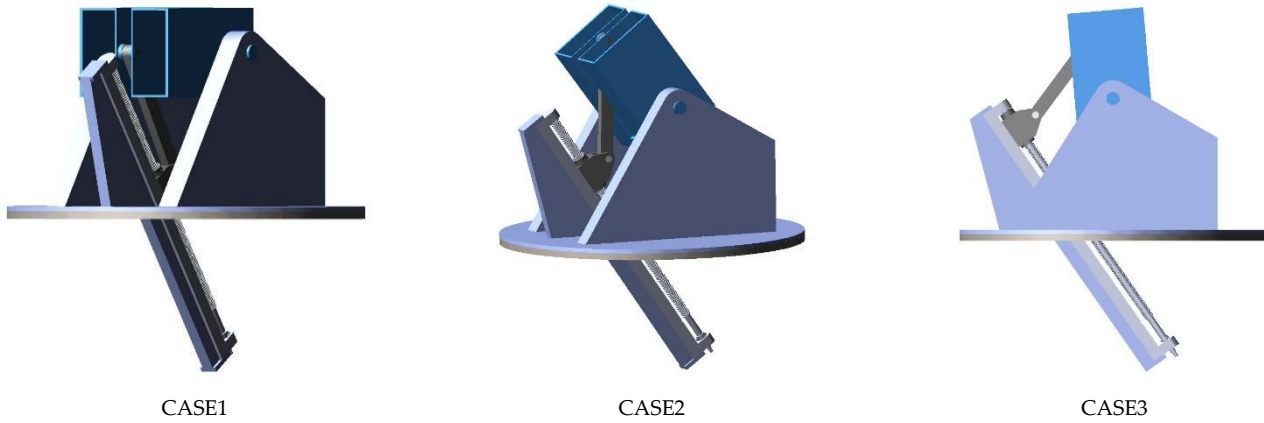


Figure 2. Schematic diagram of three emission angles

4.3. Establishment of Launcher Bracket Optimization model

In the multi-stiffness topology optimization of the launch device bracket, two extreme sub-loading conditions and one common sub-loading condition were considered, as detailed in **Table 1**. The element mesh length was set to 15 mm, and the maximum loads on the bracket under the three sub-loading conditions were applied to the trunnion area via coupling points. The outer edge of the lower plane of the bracket disk was fixed in place. The material for the bracket is selected as ordinary welded steel plate, with a density of 7.8×10^{-9} t/mm³, an elastic modulus of 2.1×10^5 MPa, and a Poisson's ratio of 0.3. The structure of the model is shown in **Figure 3**. The gray areas represent the frozen regions, which cannot be optimized. The green areas indicate the non-frozen regions, which are available for optimization design.

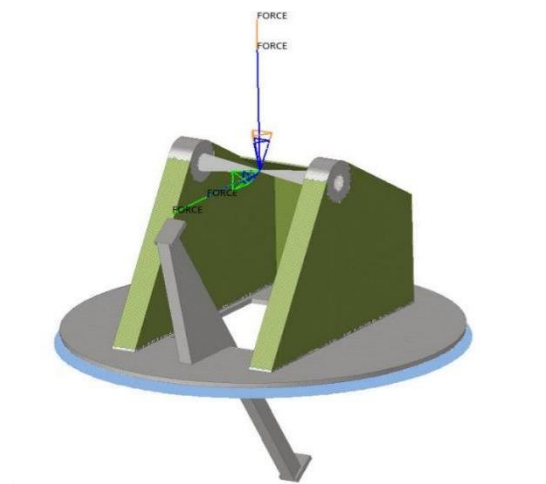


Figure 3. Optimization model of bracket.

5. Optimized Design of Launcher Bracket Structure

5.1 The Structural Compliance Optimization of the Launch Device Bracket under Multiple Loading Conditions

In the static compliance topology optimization of the launch device bracket, three different sub-loading conditions were considered. The structural strain energy weights

under these conditions were continuously adjusted by the satisfaction function during the optimization process, meaning that if the strain energy objective for a particular condition was unsatisfactory, its weight in the overall objective would be increased. Using the multi-stiffness topology optimization model constructed above, the topology optimization results for equal-weight compliance under multiple loading conditions were obtained, from which C_k^{\max} and C_k^{\min} for the three conditions can be derived. The topology structure is shown in **Figure 4**:

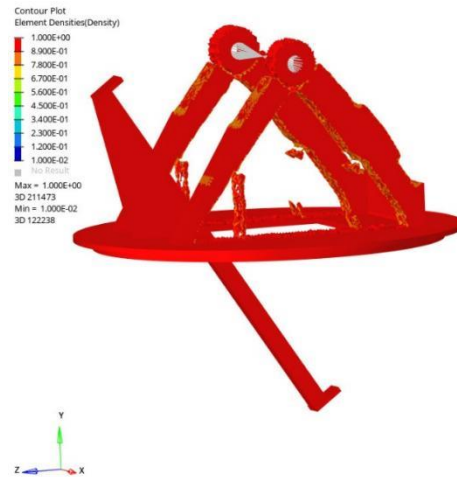


Figure 4. Multi-stiffness topology optimization results

5.2. The First Two Natural Frequencies of the Launcher Bracket Structure are Optimized

To achieve better optimization results, the optimization focuses on the first two natural frequencies. In this process, the weights of the first two natural frequencies are also set to the same value. Then, based on the average frequency formula constructed above, the average frequency of the first two orders is optimized to obtain Λ_{\max} and Λ_{\min} for the average frequency. **Figure 5** shows the specific form of the topology structure optimized for dynamic frequency.

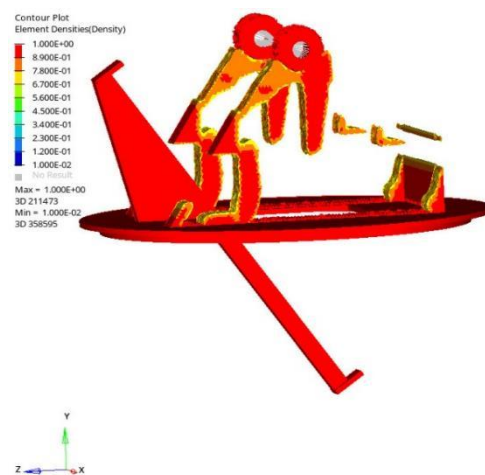


Figure 5. Optimization results of average frequency

5.3. Comprehensive Topology Optimization of Launcher Bracket Structure

Based on the topology optimization model of the bracket proposed above, along with the multi-stiffness and average frequency formulas, the topology optimization of strain

energy under three sub-loading conditions was first performed, obtaining the optimal solutions for strain energy under the three conditions and the corresponding strain energy values C_k^{\max} and C_k^{\min} . Next, frequency optimization calculations were conducted, resulting in the optimal solution for the average frequency $\Lambda(x)$ and the corresponding Λ_{\max} and Λ_{\min} values. Finally, considering both stiffness and frequency in a multi-objective scenario, an adaptive weight adjustment method was employed, and the optimal topology structure as shown in **Figure 6** was obtained.

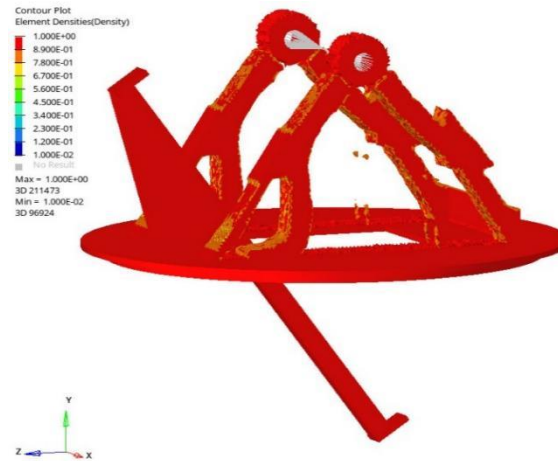


Figure 6. Comprehensive topology optimization results

5.4 Structural Design of Launcher Bracket

By analyzing **Figure 5**, it can be observed that the topology-optimized model still exhibits residual material and uneven surfaces. To achieve a bracket structure that meets the actual machining conditions and application requirements, and to ensure a more coherent bracket model, the topology results were smoothed and re-modeled. This process yielded a clearer bracket structure that satisfies both the multi-condition static stiffness requirements and the dynamic natural frequency requirements. The details are shown in **Figure 7**.

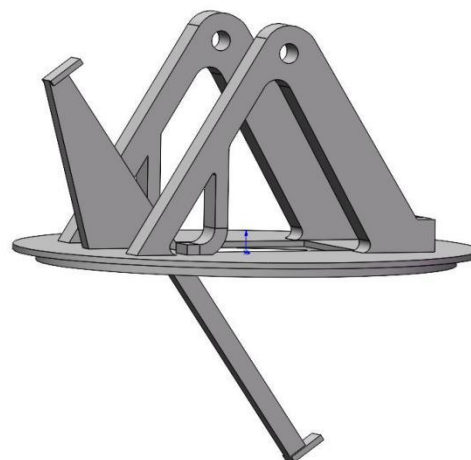


Figure 7. Bracket structure reconstructed based on topology optimization results

6. Results and Analysis

6.1. Multi-objective Topology Optimization Results

The iterative process of the first two natural frequency objectives for the optimized topology structure is shown in **Figure 8**. The iterative process of the strain energy objective is shown in **Figure 9**. As can be seen from Figures 8 and 9, the first two natural frequencies have increased, and the strain energy in all three sub-loading conditions has decreased.

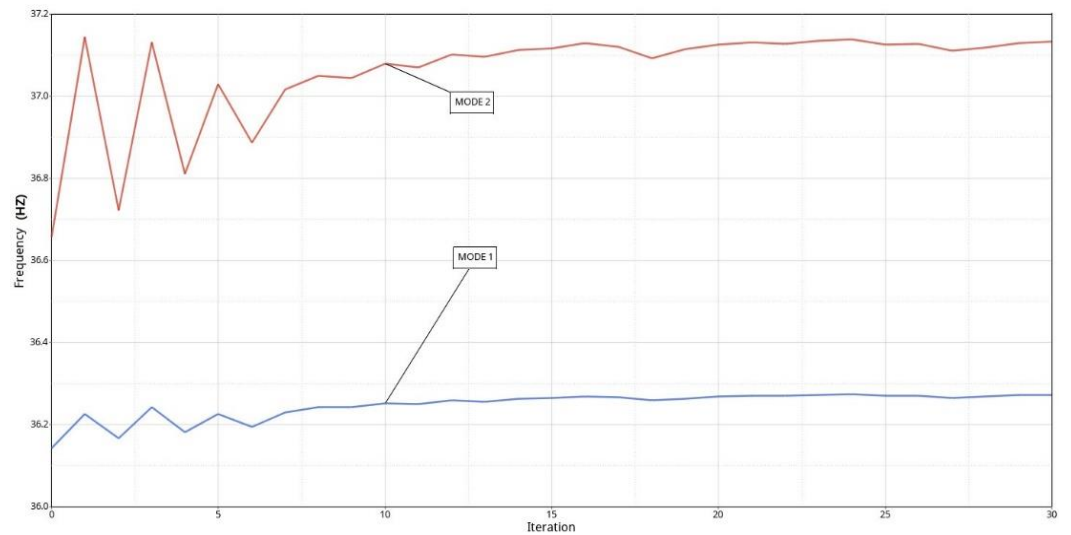


Figure 8. Frequency iteration curve

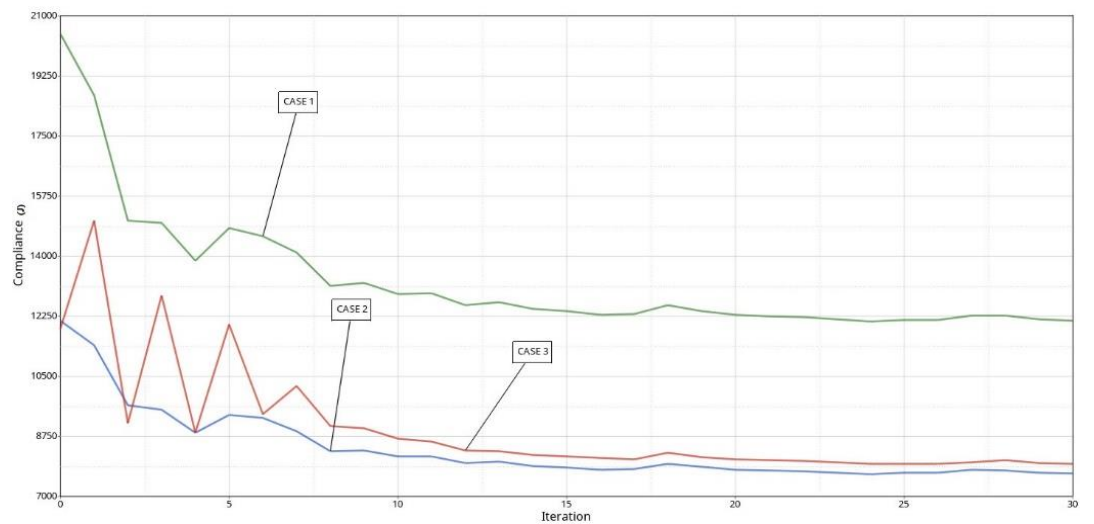
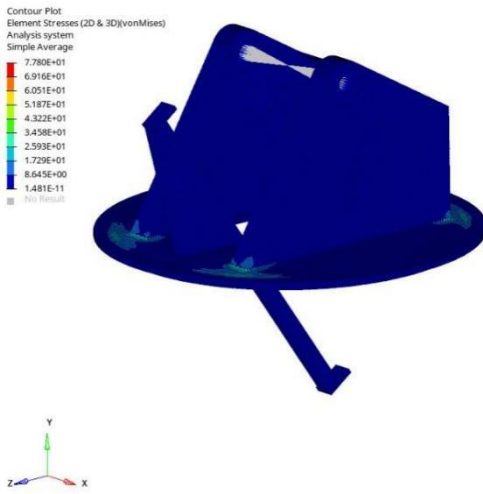


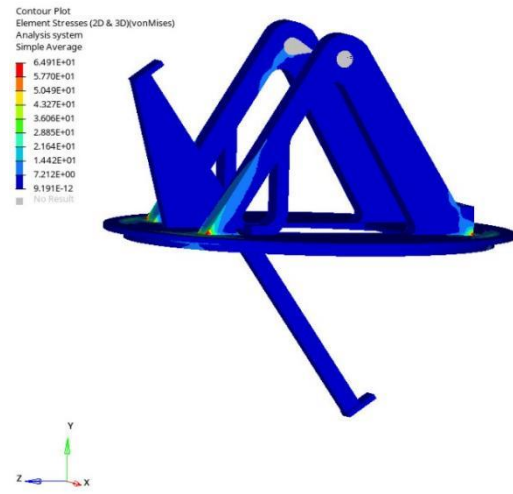
Figure 9. Iteration curves of strain energy under three ing conditions

6.2. Verification of finite element analysis

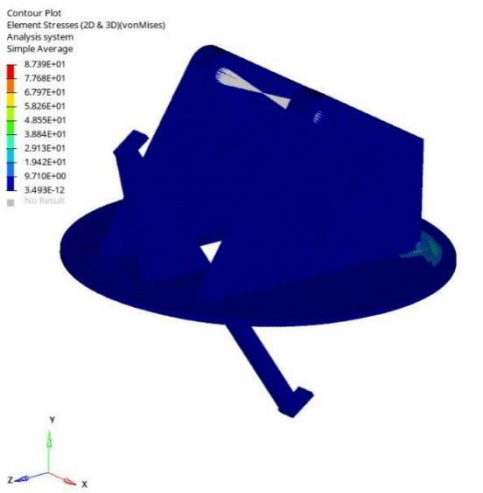
Static finite element analysis was performed, and the stress distribution is shown in **Figure 10**.



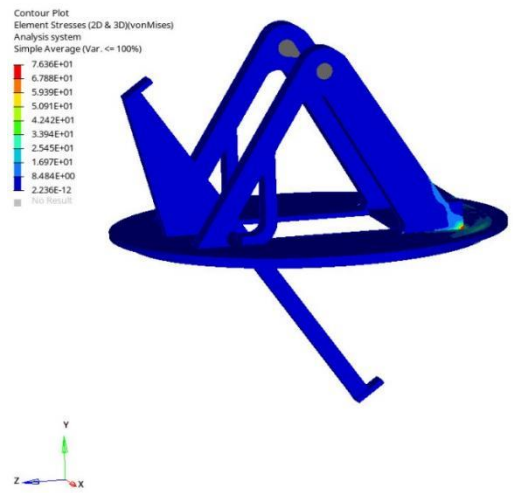
Stress distribution at 0° emission Angle of the original model



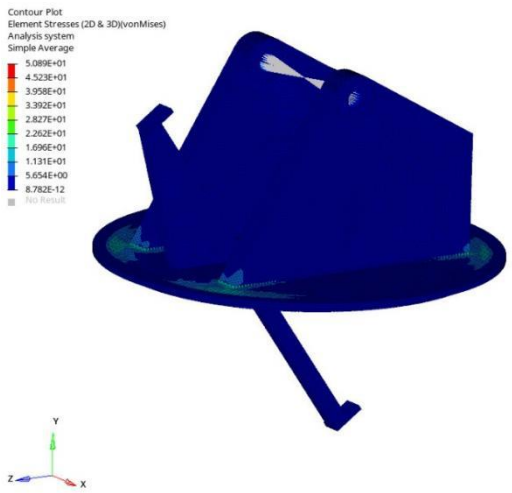
Stress distribution at 0° emission Angle of the new model



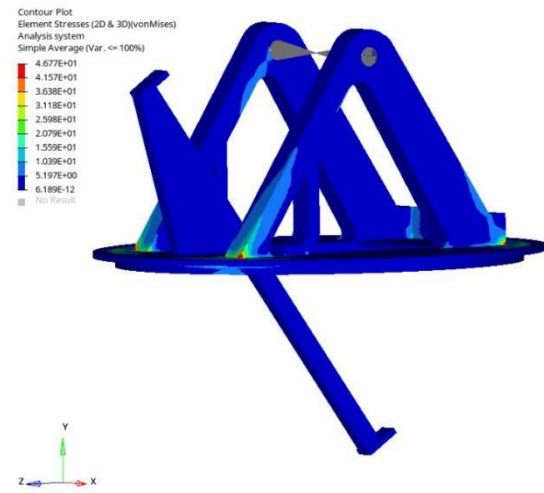
Stress distribution at 53° emission Angle of the original model



Stress distribution at 53° emission Angle of the new model



Stress distribution at 85° emission Angle of the original model



Stress distribution at 85° emission Angle of the new model

Figure 10. The stress distribution of the model before and after optimization under three ing conditions

The comparisons of strain energy and frequency before and after optimization are shown in **Table 2** and **Table 3**, respectively. The comparisons of stress and mass of the structure before and after optimization are shown in **Table 4** and **Table 5**, respectively.

Table 2. Comparison of strain energy of the structure before and after optimization

load cases	Pre-optimization strain energy	Optimized strain energy	Comparison before and after optimization
CASE1	20476	12103	Down 40.9%
CASE2	12000	7944	Down 33.8%
CASE3	12127	7656	Down 36.9%

Table 3. Frequency comparison of structures before and after optimization

	Pre-optimization frequency	Optimized frequency	Comparison before and after optimization
Mode1	36.1	36.3	Up 0.5%
Mode2	36.6	37.2	Up 1.6%

Table 4. Comparison of maximum stress before and after optimization

load cases	Maximum stress before optimization	Maximum stress after optimization	Comparison before and after optimization
CASE1	77.8	64.9	Down 16.6%
CASE2	87.4	76.4	Down 12.6%
CASE3	50.9	46.8	Down 8.1%

Table 5. Comparison of structure mass before and after optimization

	Pre-optimization quality	Optimized quality	Comparison before and after optimization
Mass	4125kg	2395kg	Down 41.9%

By comparing the data in the four tables above, it can be clearly observed that the compliance of the optimized bracket is reduced by 36.9% to 40.9%; the first two natural frequencies are increased by 0.5% to 1.6%; the maximum stress is decreased by 8.1% to 16.6%; and the structural mass is reduced by 41.9%. These results demonstrate that the improved bracket achieves greater stiffness, higher natural frequencies, and weight reduction.

7. Conclusion

To address the problem of maximizing stiffness and natural frequency as well as achieving weight reduction for a launch device bracket under multiple loading conditions, a compromise multi-objective topology optimization method with penalty factors and satisfaction-adjusted sub-loading condition weights was employed. This approach successfully obtained a comprehensive objective function that simultaneously maximizes stiffness and natural frequency. Consequently, the bracket structure was redesigned based on the optimized topology model.

Static analysis revealed that the stiffness of the newly designed bracket structure increased by nearly 60%, the first two natural frequencies increased by 0.5% to 1.6%, the mass was reduced by 41.9%, and the maximum stress decreased by 8.1% to 16.6%. This demonstrates that the compromise programming method is effective for multi-objective

topology optimization design of such launch device brackets. Additionally, this method can be referenced for the optimization design of other components of the launch device.

References

1. Su, C., Yang, L., Hao, W., et al. The Research on Multi-Objective Topology Optimization of Aircraft Engine Pylon. *Journal of Machinery Design & Manufacture*, 2020, (12), 24-27. <https://doi.org/10.3969/j.issn.1001-3997.2020.12.006>
2. Pan, X., Rong, Z., Guo, F., et al. Multi-objective topology optimization design for common base of large diesel-electric units. *Journal of Construction Machinery and Equipment*, 2024, 55, 132-136. <https://doi.org/10.3969/j.issn.1000-1212.2024.03.026>
3. Sun, X., Ding, X. Research on Multi-objective Topology Optimization Design Methods for Structure. *Journal of Machine Design and Research*, 2012, 28, 1-4, 9. <https://doi.org/10.3969/j.issn.1006-2343.2012.04.001>
4. Li, W., Ming, M., Zhang, T., et al. Multimodal Multi-objective Evolutionary Algorithm Considering Global and Local Pareto Fronts. *Acta Automatica Sinica*, 2023, 49(1), 148-160. <https://doi.org/10.16383/j.aas.c220476>
5. Cui, Y., Yu, Y., Wei, M., et al. Multi-objective Topology Optimization Design of Opening Decks Using Improved Fourfold Combination Weighting Model of Game Theory. *Journal of Journal of Mechanical Engineering*, 2023, 59(9), 263-273. <https://doi.org/10.3901/JME.2023.09.263>
6. Lan, F., Zhang, H., Wang, J., et al. Study and Application of Topology Optimization Technique for Vehicle Steering Knuckles. *Journal of Automotive Engineering*. 2014, 36(4), 464-468, 490. <https://doi.org/10.3969/j.issn.1000-680X.2014.04.015>
7. Ge, S., Guo, Z., Liang, X., et al. Optimizing Multi-objective Topology of Compliant Mechanism of Field – artillery Rocket Loading System. *Journal of Mechanical Science and Technology for Aerospace Engineering*, 2022, 41(6), 922-928. <https://doi.org/10.13433/j.cnki.1003-8728.20200409>
8. Fan, W.J, Fan, Z., Su, R., et al. Research on Multi – objective Topology Optimization on Bus Chassis Frame. *Journal of China Mechanical Engineering*, 2008, 19(12), 1505-1508. <https://doi.org/10.3321/j.issn:1004-132X.2008.12.026>
9. Xiang, W., Yu, C., Wang, K., et al. Multi-objective Topology Optimization Design for a Certain Naval Gun Bracket. *Fire Control & Command Control*, 2016, 41(6), 149-152, 156. <https://doi.org/10.3969/j.issn.1002-0640.2016.06.034>
10. Yu, Z., Jiang, J., Zhen, Y., et al. A hybrid approach for multi-weapon production planning with large-dimensional multi-objective in defense manufacturing. *Journal of Engineering Manufacture*, 2014, 228(2), 302-316. <https://doi.org/10.1177/0954405413498728>
11. Zhang, Z., Zhou, L., Xu, F., et al. Multi-objective optimization of loading path for sheet hydroforming of tank bottom *Journal of Engineering Manufacture*, 2024, 238(5), 625-637. <https://doi.org/10.1177/09544054231181281>
12. Haris, M. S., Philip, S. Marcus. Bayesian optimization for mixed-variable, multi-objective problems. *Structural and Multidisciplinary Optimization*, 2022, 65, 331. <https://doi.org/10.48550/arXiv.2201.12767>
13. Zhang, J., Wang, S., Zhou, H. Manufacturable casting parts design with topology optimization of structural assemblies. *Journal of Engineering Manufacture*, 2022, 236(4), 401-412. <https://doi.org/10.1177/09544054211035067>
14. Fan, W., Xu, Z., Wu, B., et al. Structural multi-objective topology optimization and application based on the criteria importance through intercriteria correlation method. *Engineering Optimization*, 2021, 54(5), 830-846. <https://doi.org/10.1080/0305215X.2021.1901087>
15. Slesongsom, S., Bureerat, S. Multi-objective optimization of a steering linkage. *Journal of Mechanical Science and Technology*, 2016, 30(8), 3681-3691. <https://doi.org/10.1007/s12206-016-0730-4>
16. Tawatchai, K., Sujin, B. Multi-objective topology optimization using evolutionary algorithms. *Engineering Optimization*, 2011, 43(5), 541-557. <https://doi.org/10.1080/0305215X.2010.502935>
17. Marck, G., Nemer, M., Harion, J. L., et al. Topology optimization using the simp method for multiobjective conductive problems. *Numerical Heat Transfer. Part B: Fundamentals*, 2012, 61(6), 439-470. <https://doi.org/10.1080/10407790.2012.687979>

Disclaimer/Publisher's Note: The statements, opinions and data contained in all publications are solely those of the individual author(s) and contributor(s) and not of BSP and/or the editor(s). BSP and/or the editor(s) disclaim responsibility for any injury to people or property resulting from any ideas, methods, instructions or products referred to in the content.